



Cite this: *Dalton Trans.*, 2017, **46**, 6177

Received 29th March 2017,
Accepted 10th April 2017

DOI: 10.1039/c7dt01130j

rsc.li/dalton

Formation of exceptionally weak C–C bonds by metal-templated pinacol coupling†

E. Folkertsma,^a S. H. Benthem,^a L. Witteman,^a C. A. M. R. van Slagmaat,^a M. Lutz,^b R. J. M. Klein Gebbink^a and M.-E. Moret^a★

The ability of the bis(imidazolyl)ketone ligand BM^{diPh}IK (bis(1-methyl-4,5-diphenylimidazolyl)ketone) to function as a redox active ligand has been investigated. The reduction of [M(BM^{diPh}IK)Cl₂] (M = Fe and Zn) complexes resulted in a pinacol-type coupling to form dinuclear complexes featuring very weak and abnormally elongated C–C bonds (1.729(5) and 1.708(3) Å for Fe and Zn, respectively). Oxidation of these complexes using ferrocenium in the presence of Cl[−] ions regenerated the original [M(BM^{diPh}IK)Cl₂] complexes, showing the reversibility of the coupling process. This makes it a potentially interesting approach for the storage of electrons and application of the BM^{diPh}IK ligand as a redox active ligand.

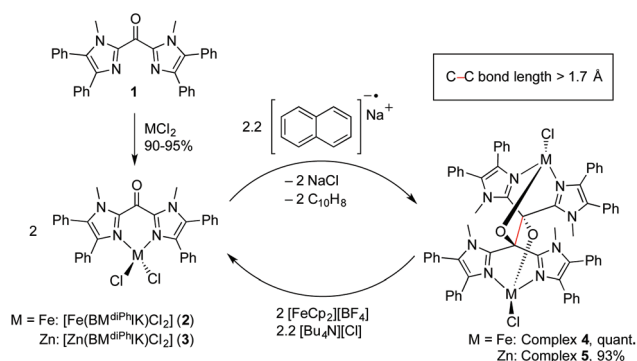
Introduction

The use of redox active ligands has emerged as a promising approach to develop efficient catalysts based on first-row transition metals.^{1a–f} These ligands can reversibly accept and release electrons during a catalytic cycle, facilitating multi-electron steps, such as oxidative addition and reductive elimination, for metals that do not readily undergo two-electron redox changes.^{1c,2} Ligand-centered redox activity often involves low-lying π*-orbitals as for example in catecholates,³ bis(imino)pyridines,^{2a,b,4} and formazanates.⁵ Redox active ligands have been successfully applied to important catalytic transformations such as hydrogenation, hydrosilylation, and aziridination.⁶ In addition, the formation of new C–C bonds *via* reductive coupling has been observed for several redox active ligands.⁷ When this process is reversible, the C–C bond can be

envisioned to function as an electron reservoir in devices such as molecular batteries.⁸

Diarylketones have long been known to exhibit reversible redox chemistry, as illustrated by the stability of the ketyl radical anion derived from benzophenone, owing to their low-lying π*-orbital stabilized by conjugation. In particular, pinacol coupling of diarylketones is usually disfavored: the benzophenone radical anion can in fact be generated by deprotonating 1,1,2,2-tetraphenylethane-1,2-diol.^{9a} From a synthetic perspective, this difficulty can be overcome by using strong Lewis acids to stabilize the pinacolate intermediate prior to protonation.^{9b–d}

On this basis, we set out to study the use of the diarylketone motif in redox active ligands. We report the coordination chemistry of the tetraphenyl-substituted bis(methylimidazolyl) ketone ligand BM^{diPh}IK (bis(1-methyl-4,5-diphenylimidazolyl) ketone, **1**) to Fe and Zn and the ligand-centered reduction of the obtained complexes (Scheme 1). The reduction of [M(BM^{diPh}IK)Cl₂] (**2**: M = Fe; **3**: M = Zn) leads to dinuclear complexes featuring exceptionally long C–C bonds. We investigate these experimentally and computationally, showing in particular that these weak C–C bonds can be oxidatively cleaved at



Scheme 1 Reductive radical coupling of two ligands coordinated to a metal chloride and oxidation back to the original mononuclear dichloride complexes.

^aOrganic Chemistry & Catalysis, Debye Institute for Nanomaterials Science, Utrecht University, Universiteitsweg 99, 3584 CG Utrecht, The Netherlands. E-mail: m.moret@uu.nl

^bBijvoet Center for Biomolecular Research, Crystal and Structural Chemistry, Utrecht University, Padualaan 8, 3584 CH Utrecht, The Netherlands

† Electronic supplementary information (ESI) available. CCDC 1519042–1519049. For ESI and crystallographic data in CIF or other electronic format see DOI: 10.1039/c7dt01130j

mild potentials, which suggests that they can act as an electron reservoir.

Results and discussion

The ligand BM^{diPh}IK (**1**) was synthesized *via* a modification of the method by Garner *et al.*¹⁰ and treated with metal dichlorides FeCl₂ or ZnCl₂ in THF to obtain pseudotetrahedral complexes [Fe(BM^{diPh}IK)Cl₂] (**2**) and [Zn(BM^{diPh}IK)Cl₂] (**3**), respectively. The ESI-MS spectra of **2** and **3** display the characteristic ions [M(BM^{diPh}IK)Cl]⁺ corresponding to the Cl[−] loss, supporting their assignment as 1 : 1 complexes. The Fe complex **2** exhibits ¹H NMR signals ranging from +43 to −7.5 ppm and an effective magnetic moment of 5.2μ_B (Evans' method), consistent with an S = 2 ground state.¹¹ Interestingly, the IR signal corresponding to the C=O stretch vibration in BM^{diPh}IK (1622 cm^{−1}) shifts to higher energies upon complexation to FeCl₂ (1647 cm^{−1}) or ZnCl₂ (1633 cm^{−1}), which is likely due to inductive effects, the metal effectively acting as an electron-withdrawing substituent on the imidazole ring. The X-ray crystal structures reveal that **2** and **3** are isostructural and have a distorted tetrahedral metal geometry with crystallographic C₂-symmetry. All Fe–N bond lengths are slightly longer than 2 Å, typical of high-spin pseudotetrahedral Fe^{II}-complexes.^{12,13}

Ligand **1** and complexes **2** and **3** were investigated by cyclic voltammetry (CV) (Fig. 1). Because of the low solubility of **2** and **3** in THF, a 0.1 M solution of Bu₄NPF₆ in MeCN was chosen as the electrolyte. The free ligand showed a quasi-reversible (*i*_{pa}/*i*_{pc} = 0.77) reductive wave with a peak potential (*E*_{pc}) of −2.10 V, close to those of the related di(2-pyridyl) ketone (*E*_{pc} = −2.00 V, *i*_{pa}/*i*_{pc} = 0.71) and benzophenone (*E*_{pc} = −2.23 V, *i*_{pa}/*i*_{pc} = 0.88). This reductive wave corresponds to the formation of a ketyl radical anion, which could also be gener-

ated by reaction with sodium in THF and observed by EPR with a *g*-value of 2.004 and a complex hyperfine pattern typical of diarylketyl radicals¹⁴ (see the ESI† for details). Iron complex **2** displays an irreversible reduction wave with *E*_{pc} = −1.48 V, and the Zn analogue **3** displays a similar irreversible wave at −1.52 V. Since no metal-centered redox processes are expected for the d¹⁰ Zn center, these processes are assigned to ligand-centered reductions facilitated by coordination to a Lewis acidic metal center. Their irreversible character likely stems from the loss of a halide upon reduction, even though neither the use of a chloride-containing electrolyte (0.1 M Bu₄NCl in MeCN) nor variation of the scan rate did increase the reversibility. In addition, an intense irreversible oxidative wave is observed at +0.54 V for the Fe complex **2**. It is also observed in a CV of **2** starting in the oxidative direction, but is absent in the CV of the Zn analogue **3**. Therefore, we assign this wave to the Fe(II/III) couple. Additional irreversible oxidation processes of lower intensity were observed at −0.32 and 0.15 V for **2** and at −0.25, 0.04, and 1.07 V for **3**, which were tentatively assigned to oxidation processes related to species that were formed at reductive potentials, *e.g.* *via* partial degradation.

Having observed ligand-centered reduction events at accessible potentials for complexes **2** and **3**, we sought to isolate the corresponding reduction products. First, the reduction of complex **2** with sodium naphthalenide quantitatively afforded the colorless compound **4**. The ¹H NMR spectrum of **4** displays seven paramagnetically broadened peaks ranging from −7.9 to 9.6 ppm suggesting that all imidazole moieties are magnetically equivalent. In the IR spectrum, both in CH₂Cl₂ solution and as a solid, the original C=O vibration is no longer present. Instead, two strong bands appeared at 1175 and 560 cm^{−1}, which are consistent with ν(C–O) and ν(M–O), respectively, of a coordinating alkoxide,¹⁵ suggesting the formation of a pinacolate structure.

The structure of **4** was elucidated by X-ray crystallography (Fig. 2) as a dinuclear pinacolate complex in which each alkoxy-group coordinates to the Fe center that initially belonged to a second complex, effectively acting as a facial *N,N,O*-ligand to the Fe centers.^{1,16} The asymmetric unit contains two independent molecules; in the first one, an additional chloride ligand completes the pseudotetrahedral coordination environment of both Fe centers, while the second one incorporates an additional THF molecule on one of the Fe centers and suffers from additional disorder (see the ESI† for details). For clarity metric parameters are only discussed for the first molecule. The Fe–N (2.084(5), 2.094(4), 2.098(5), and 2.090(4) Å) and Fe–Cl (2.2190(18), and 2.2224(18) Å) bond lengths are rather similar to the distances found in the starting complex **2** and the Fe–O distances of 1.918(4)/1.906(4) Å are common for a tetrahedral high-spin Fe^{II}-complex. The large distance between the two Fe centers (5.7361(11) Å) suggests at most weak magnetic coupling, in accord with a solution effective magnetic moment of 6.4μ_B, (Evans' method), close to the value of 6.9μ_B that is expected for two non-interacting S = 2 centers.¹⁷ The most salient structural feature of compound **4**, however, is the exceptionally long

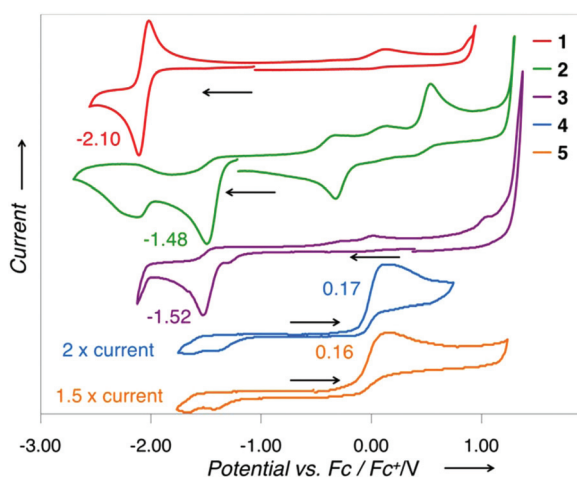


Fig. 1 Cyclic voltammograms of compounds **1** (2.0 mM), **2** (2.8 mM), **3** (1.3 mM), **4** (saturated) and **5** (saturated) in 0.1 M Bu₄NPF₆ in MeCN, referenced vs. ferrocene at a scan rate of 100 mV s^{−1}. The arrows indicate the starting points and scanning directions.

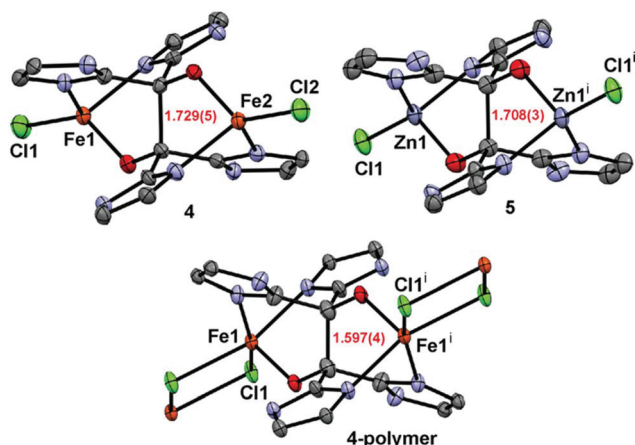


Fig. 2 Molecular structures of complexes **4** and **5** in the crystal.²⁷ Hydrogen atoms, substituents on the imidazole rings, and co-crystallized (solvent) molecules have been omitted for clarity. Displacement ellipsoids are drawn at the 50% probability level. Colors: gray: C; light blue: N; red: O; green: Cl; orange: Fe; purple: Zn. The length of the central C–C bond (in Å) is indicated in red. Symmetry code *i*: [1 – *x*; 1 – *y*; 1 – *z*].

pinacolate C–C bond length of 1.729(5) Å,¹⁸ which suggests an extremely weak bond (*vide infra*).

Interestingly, slightly different crystallization conditions for **4** afforded a coordination polymer in which two Fe centers are linked by two bridging chloride ligands, resulting in a 5-coordinate environment best described as a square pyramid ($\tau = 0.04$) with the oxygen atom as the apex (Fig. 2). Remarkably, the central C–C bond in that polymer is considerably shorter (1.597(4) Å), showing that this bond is sensitive to the coordination environment of the metal. This effect is most likely due to mechanical transmission of geometrical changes at Fe through the cage structure. More specifically, moving from a 4- to a 5-coordinate geometry results in a decrease in the sum of N–Fe–N and N–Fe–O angles from 269.2(3)° and 269.7(3) to 264.97(13)°, allowing for a more compact geometry with a shorter C–C bond.

The coupling reaction also proceeds with a redox-inactive divalent metal center: the reaction of sodium naphthalenide with **3** afforded the analogous dinuclear Zn complex **5** as a white solid in 93% yield. The ¹³C NMR spectrum of **5** displays a distinctive peak corresponding to the two identical quaternary alkoxide carbons at 89.8 ppm, which is comparable to other pinacolate complexes.¹⁹ The IR spectrum displays two diagnostic signals for coordinating alkoxide groups: $\nu(\text{C–O})$ and $\nu(\text{M–O})$ at 1180 and 546 cm^{–1}, respectively. The molecular structure of **5** in the crystal is very similar to that of the Fe analogue **4**. The central C–C bond is only slightly shorter (1.708(3) Å), suggesting that the abnormal C–C bond length is a general property of this structural motif.

Demetallation of **4** and **5** with ethylenediaminetetraacetic acid disodium salt (EDTA) in a biphasic CH₂Cl₂/H₂O mixture under oxygen-free conditions results in a disproportionation reaction, which is probably due to the lability of the central

C–C bond. The isolated organic material (>85% yield) mainly consisted of BM^{diph}IK (~50%) and the corresponding alcohol H-BM^{diph}IA (~35%) together with a third, unidentified minor species (~10%). This observation suggests a key role of the metal ions in controlling the reductive coupling of the ketone functionalities, as has been observed in related iron-^{20,21} and lanthanide-based^{22c} systems.

The very weak character of the central C–C bonds in **4** and **5** is also apparent in their electrochemical behavior. The cyclic voltammograms of **4** and **5** both display an irreversible oxidation with low peak potentials of 0.16 and 0.17 V, respectively (Fig. 1), indicating a ligand-based process that should be chemically accessible with a mild oxidant. Additionally, weaker reductive waves around –1.5 V appear after cycling through the oxidative region suggesting that some species containing the ketone-ligand are formed upon oxidation. This was confirmed by chemical oxidation of **4** and **5** with 2 eq. of [Fe^{III}Cp₂][BF₄] in the presence of 2.2 eq. of [Bu₄N][Cl] to yield the mononuclear complexes **2** and **3**, respectively, as the only products in quantitative yields. Thus, the weak C–C bond in both **4** and **5** can be oxidized at mild potentials, in contrast with the strong oxidants periodic acid (Malaprade) and lead tetraacetate (Criegee) used in standard procedures for the cleavage of vicinal diols.²³

Intrigued by the exceptionally long C–C bonds found in **4** and **5**, we studied the diamagnetic Zn compound **5** using density functional theory (DFT) and Natural Bond Orbital (NBO) analysis (see the ESI† for details). A relaxed potential energy surface (PES) scan along the C–C distance in the singlet state finds a minimum in energy at 1.73 Å with an NBO Wiberg bond index of 0.77, in good agreement with the experimental value of 1.708(3) Å (Fig. 3, diamonds). Upon elongation of the bond a second minimum is found at 2.65 Å, indicating

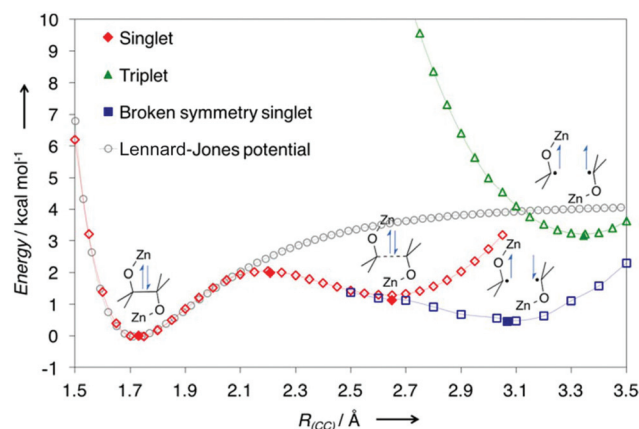


Fig. 3 Relaxed potential energy surface scan of the singlet state (diamonds), the broken symmetry singlet state (squares), and the triplet state (triangles) of **5** using (U)B3LYP and 6-31g** for C, H, N, O, and Cl and LANL2DZ (basis set and pseudopotential) for Zn. As a comparison, a Lennard-Jones fit for the bound structure is included (circles). The filled symbols indicate local minima or transition states that were optimized without any constraints. A line connecting the data points is added as guide to the eye. Energy differences are relative to the optimized singlet state (minimum in diamonds).

a very weak C–C interaction. Envisioning that the corresponding unbound state may be better described as a diradical (Fig. 3, squares), we optimized the structure as a broken-symmetry singlet, which yielded a C–C distance of 3.07 Å and a Wiberg bond order of only 0.05. These two states are connected by a transition state structure at $R_{\text{CC}} = 2.21$ Å at an energy barrier of 2.2 kcal mol^{−1}. The related triplet state shows an even longer C–C distance of 3.34 Å which lies only 3.2 kcal mol^{−1} above the ground state, indicating weak coupling in the dissociated state (Fig. 3, triangles).

Estimating the bond dissociation energy (BDE) of bonds included in a cage system is difficult because of strong coupling with other bonds, such as the Zn–O coordination bonds in **5**. Interestingly, the short-distance region ($R_{\text{CC}} = 1.5$ – 2.1 Å) of the PES could be well represented by a Lennard-Jones potential with an equilibrium distance (r_m) of 1.72 Å and a depth of the potential well (ϵ) of 4.2 kcal mol^{−1}, which can be seen as an approximate measure of the BDE. It is in rough agreement with the empirical relationship between the bond length and BDE proposed by Zavitsas *et al.*,²⁴ which yields only slightly larger BDEs of 8 and 17 kcal mol^{−1} for **4** and **5**, respectively.

Additional calculations shed some light on the origin of the C–C bond elongation. First, steric repulsion between phenyl substituents appears to play a marginal role at most, since replacing all Ph groups with H atoms in **5** results in a very similar relaxed PES scan (see the ESI†). In contrast, the PES of the protonated pinacol ligand exhibits a single energy minimum at a shorter bond length of 1.65 Å, suggesting that a more electron rich oxygen atom contributes to weakening of the C–C bond. A rationale for this effect is provided by NBO analysis performed on the ground-state structure with a C–C distance of 1.73 Å (Fig. 4): second-order perturbation analysis reveals significant donation (14.5 kcal mol^{−1}) of the lone pair p-orbital on the oxygen atoms into the σ^* -orbital of the C–C bond. This hyperconjugation effect, complemented by weaker donation (<6.4 kcal mol^{−1}) from the σ -orbital of the C–C bond into the $\sigma^*(\text{C–N})$ orbitals of the imidazole rings, electronically weakens the C–C bond. Finally, the full dissociation of **5** into monomeric ketyl radical/ZnCl complexes is calculated to be 45.4 kcal mol^{−1}, indicating that the Zn–O interactions contri-

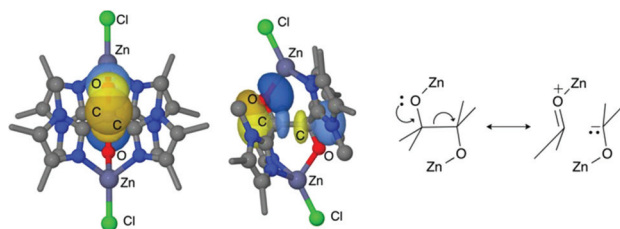


Fig. 4 Left: Visualization of the pre-orthogonalized NBOs (front and side views) depicting the donation of the lone pair in the p-orbital of the oxygen into the anti-bonding σ^* -orbital of the central C–C bond in the singlet state of **5**. Ph-Substituents and hydrogen atoms are omitted for clarity. Right: Resonance-structure depiction of this hyperconjugation interaction.

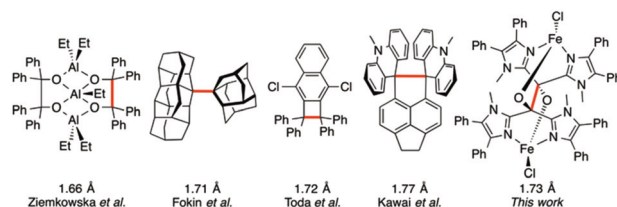


Fig. 5 Examples of molecules in the literature with long C–C bonds.^{19a,25}

bute to the stability of the dinuclear structure more than the C–C bond.

The C–C bonds in **4** (1.729(5) Å) and **5** (1.708(3) Å) are abnormally long; the expected Csp^3 – Csp^3 bond length is 1.53 Å, and pinacolate-type C–C bonds range between 1.56 and 1.66 Å.^{19a,22} A few examples of Csp^3 – Csp^3 bond lengths above 1.70 Å are known, including a single example by Kawai *et al.* in which the bond is longer (1.77 Å) than that in **4** (Fig. 5). Commonly, steric hindrance and/or strain causes the elongation of the bond while the overall stability is maintained by a second, supporting, interaction which can be strong covalent bonds²⁵ or weaker London dispersion forces.²⁶ In compounds **4** and **5**, this role is assumed by coordination bonds.

Conclusions

In conclusion, we have shown that pinacolate moieties with extremely long C–C bonds (>1.7 Å) can be prepared by the reduction of iron and zinc complexes of the bis-imidazolyl-ketone ligand BM^{diPh}IK. Metal coordination facilitates the reduction by *ca.* 0.7 V and contributes to stabilizing the weak C–C bond in the obtained cage structure. DFT calculations indicate that the long C–C bond arises from the energetic proximity of a diradical state in which the bond is broken. Weak C–C bonds arising from the reductive coupling of [M(salophen)] or from the oxidative coupling of pyrrolide ligands have been proposed as a means to store redox equivalents in molecular batteries.⁸ In this context, it is particularly interesting that the central C–C bond can be (electro)chemically oxidized at mild potentials, suggesting that these weak pinacol bonds could be used to reversibly store electrons, *e.g.* during a catalytic cycle. Studies in this direction are underway in our laboratories.

Acknowledgements

The authors would like to thank the Dutch National Research School Combination-Catalysis Controlled by Chemical Design (NRSC-Catalysis) for their financial support. M.-E. M. acknowledges funding from the European Union Seventh Framework Programme (FP7/2007–2013) under grant agreement PIFI-GA-2012-327306 (IIF-Marie Curie grant) and Utrecht University (Tenure-track grant, Sectorplan Natuur-en

Scheikunde). The DFT work was carried out on the Dutch national e-infrastructure with the support of the SURF Foundation. The X-ray diffractometer has been financed by the Netherlands Organization for Scientific Research (NWO).

References

- (a) S. Blanchard, E. Derat, M. Desage-El Murr, L. Fensterbank, M. Malacria and V. Mouries-Mansuy, *Eur. J. Inorg. Chem.*, 2012, 376–389; (b) J. I. van der Vlugt, *Eur. J. Inorg. Chem.*, 2012, 363–375; (c) J. R. Khusnutdinova and D. Milstein, *Angew. Chem., Int. Ed.*, 2015, **54**, 12236–12273; (d) W. Kaim and B. Schwederski, *Coord. Chem. Rev.*, 2010, **254**, 1580–1588; (e) O. R. Luca and R. H. Crabtree, *Chem. Soc. Rev.*, 2013, **42**, 1440–1459; (f) V. Lyaskovskyy and B. de Bruin, *ACS Catal.*, 2012, **2**, 270–279.
- (a) P. J. Chirik and K. Wieghardt, *Science*, 2010, **327**, 794–795; (b) S. C. Bart, E. Lobkovsky and P. J. Chirik, *J. Am. Chem. Soc.*, 2004, **126**, 13794–13807; (c) W. I. Dzik, J. I. van der Vlugt, J. N. H. Reek and B. de Bruin, *Angew. Chem., Int. Ed.*, 2011, **50**, 3356–3358.
- S. N. Brown, *Inorg. Chem.*, 2012, **51**, 1251–1260.
- (a) B. D. Stubbert, J. C. Peters and H. B. Gray, *J. Am. Chem. Soc.*, 2011, **133**, 18070–18073; (b) S. C. Bart, K. Chłopek, E. Bill, M. W. Bouwkamp, E. Lobkovsky, F. Neese, K. Wieghardt and P. J. Chirik, *J. Am. Chem. Soc.*, 2006, **128**, 13901–13912; (c) A. M. Tondreau, C. C. H. Atienza, K. J. Weller, S. A. Nye, K. M. Lewis, J. G. P. Delis and P. J. Chirik, *Science*, 2012, **335**, 567–570; (d) B. de Bruin, E. Bill, E. Bothe, T. Weyhermuller and K. Wieghardt, *Inorg. Chem.*, 2000, **39**, 2936–2947.
- (a) M. Chang, P. Roewen, R. Traviso-Puente, M. Lutz and E. Otten, *Inorg. Chem.*, 2015, **54**, 379–388; (b) M. C. Chang, T. Dann, D. P. Day, M. Lutz, G. G. Wildgoose and E. Otten, *Angew. Chem., Int. Ed.*, 2014, **53**, 4118–4122.
- (a) E. R. King, E. T. Hennessy and T. A. Betley, *J. Am. Chem. Soc.*, 2011, **133**, 4917–4923; (b) C. Cheng and J. F. Hartwig, *Chem. Rev.*, 2015, **115**, 8946–8975; (c) J. M. Hoyt, V. A. Schmidt, A. M. Tondreau and P. J. Chirik, *Science*, 2015, **349**, 960–963; (d) P. O. Lagaditis, P. E. Sues, J. F. Sonnenberg, K. Y. Wan, A. J. Lough and R. H. Morris, *J. Am. Chem. Soc.*, 2014, **136**, 1367–1380.
- (a) J. Jastrzebski, J. M. Klerks and G. Van Koten, *J. Organomet. Chem.*, 1981, **210**, C49–C53; (b) G. Van Koten, J. T. B. H. Jastrzebski and K. Vrieze, *J. Organomet. Chem.*, 1983, **250**, 49–61; (c) E. Gallo, E. Solari, N. Re, C. Floriani, A. Chiesi-Villa and C. Rizzoli, *J. Am. Chem. Soc.*, 1997, **119**, 5144–5154; (d) T. W. Myers, N. Kazem, S. Stoll, R. D. Britt, M. Shanmugam and L. A. Berben, *J. Am. Chem. Soc.*, 2011, **133**, 8662–8672; (e) D. Zhu, I. Thapa, I. Korobkov, S. Gambarotta and P. H. M. Budzelaar, *Inorg. Chem.*, 2011, **50**, 9879–9887; (f) B. P. Jacobs, P. T. Wolczanski and E. B. Lobkovsky, *Inorg. Chem.*, 2016, **55**, 4223–4232; (g) B. A. Frazier, V. A. Williams, P. T. Wolczanski, S. C. Bart, K. Meyer, T. R. Cundari and E. B. Lobkovsky, *Inorg. Chem.*, 2013, **52**, 3295–3312.
- (a) F. Franceschi, E. Solari, R. Scopelliti and C. Floriani, *Angew. Chem., Int. Ed.*, 2000, **39**, 1685–1687; (b) C. Floriani, E. Solari, F. Franceschi, R. Scopelliti, P. Belanzoni and M. Rosi, *Chem. – Eur. J.*, 2001, **7**, 3052–3061; (c) K. Venkatesan, O. Blacque and H. Berke, *Organometallics*, 2006, **25**, 5190–5200.
- (a) M. Zalibera, P. Nesvadba and G. Gescheidt, *Org. Lett.*, 2013, **15**, 4627–4629; (b) J. S. Wang, J. T. Li, Z. P. Lin and T. S. Li, *Synth. Commun.*, 2006, **35**, 1419–1424; (c) H. Kronenwetter, J. Husek, B. Etz, A. Jones and R. Manchanayakage, *Green Chem.*, 2014, **16**, 1489–1495; (d) A. Yoshimura, T. Saeki, A. Nomoto and A. Ogawa, *Tetrahedron*, 2015, **71**, 5347–5355.
- (a) J. McMaster, R. L. Beddoes, D. Collison, D. R. Eardley, M. Helliwell and C. D. Garner, *Chem. – Eur. J.*, 1996, **2**, 685–693; (b) P. Lucas, N. E. Mehdi, H. A. Ho, D. Bélanger and L. Breau, *Synthesis*, 2000, 1253–1258.
- (a) D. F. Evans, *J. Chem. Soc.*, 1959, 2003–2005; (b) G. J. P. Britovsek, V. C. Gibson, S. K. Spitzmesser, K. P. Tellmann, A. J. P. White and D. J. Williams, *J. Chem. Soc., Dalton Trans.*, 2002, 1159–1171.
- E. Folkertsma, E. F. de Waard, G. Korpershoek, A. J. van Schaik, N. Solozabal Mirón, M. Borrmann, S. Nijse, M. A. H. Moelands, M. Lutz, M. Otte, M.-E. Moret and R. J. M. Klein Gebbink, *Eur. J. Inorg. Chem.*, 2016, 1319–1332.
- F. A. Jové, C. Pariya, M. Scoblete, G. P. A. Yap and K. H. Theopold, *Chem. – Eur. J.*, 2011, **17**, 1310–1318.
- L. Nadjo and J. M. Savéant, *J. Electroanal. Chem. Interfacial Electrochem.*, 1971, **30**, 41–57.
- K. Nakamoto, *Infrared and Raman Spectra of Inorganic and Coordination Compounds, Part B, Applications in Coordination, Organometallic, and Bioinorganic Chemistry*, John Wiley & Sons, Inc., 6th edn, 2009.
- (a) M. A. H. Moelands, S. Nijse, E. Folkertsma, B. de Bruin, M. Lutz, A. L. Spek and R. J. M. Klein Gebbink, *Inorg. Chem.*, 2013, **52**, 7394–7410; (b) P. C. A. Bruijninx, G. van Koten and R. J. M. Klein Gebbink, *Chem. Soc. Rev.*, 2008, **37**, 2716–2744.
- B. Weber and E. Kaps, *Heteroat. Chem.*, 2005, **16**, 391–397.
- W. M. Haynes, *CRC Handbook of Chemistry and Physics*, CRC press, 96th edn, 2015.
- (a) W. Ziemkowska, S. Kucharski, A. Kołodziej and R. Anulewicz-Ostrowska, *J. Organomet. Chem.*, 2004, **689**, 2930–2939; (b) M. J. Tomaszewski and J. Warkentin, *J. Chem. Soc., Chem. Commun.*, 1993, **53**, 1407–1408.
- R. Siebenlist, H. Frühauf, K. Vrieze, W. J. J. Smeets and A. L. Spek, *Eur. J. Inorg. Chem.*, 2000, 907–919.
- A. De Cian, R. Weiss, Y. Chauvin, D. Commereuc and D. Hugo, *J. Chem. Soc., Chem. Commun.*, 1976, 249–250.
- (a) S. G. Bott, A. P. Marchand and Z. Liu, *J. Chem. Crystallogr.*, 1995, **25**, 417–420; (b) W. Ziemkowska,

- R. Anulewicz-Ostrowska and M. Cyrański, *Polyhedron*, 2008, **27**, 962–968; (c) Z. Hou, A. Fujita, Y. Zhang, T. Miyano, H. Yamazaki and Y. Wakatsuki, *J. Am. Chem. Soc.*, 1998, **120**, 754–766; (d) I. L. Fedushkin, A. A. Skatova, V. K. Cherkasov, V. A. Chudakova, S. Dechert, M. Hummert and H. Schumann, *Chem. – Eur. J.*, 2003, **9**, 5778–5783; (e) Z. Hou, T. Miyano, H. Yamazaki and Y. Wakatsuki, *J. Am. Chem. Soc.*, 1995, **117**, 4421–4422; (f) L. Tahsini, S. E. Specht, J. S. Lum, J. J. M. Nelson, A. F. Long, J. A. Golen, A. L. Rheingold and L. H. Doerrer, *Inorg. Chem.*, 2013, **52**, 14050–14063; (g) K. Isele, F. Gigon, A. F. Williams, G. Bernardinelli, P. Franz and S. Decurtins, *Dalton Trans.*, 2007, 332–341.
- 23 (a) B. H. Nicolet and L. A. Shinn, *J. Am. Chem. Soc.*, 1939, **61**, 1615–1615; (b) E. Baer, J. M. Grosheintz and H. O. L. Fischer, *J. Am. Chem. Soc.*, 1939, **61**, 2607–2609.
- 24 A. A. Zavitsas, *J. Phys. Chem. A*, 2003, **107**, 897–898.
- 25 (a) A. A. Fokin, L. V. Chernish, P. A. Gunchenko, E. Y. Tikhonchuk, H. Hausmann, M. Serafin, J. E. P. Dahl, R. M. K. Carlson and P. R. Schreiner, *J. Am. Chem. Soc.*, 2012, **134**, 13641–13650; (b) K. K. Baldridge, Y. Kasahara, K. Ogawa, J. S. Siegel, K. Tanaka and F. Toda, *J. Am. Chem. Soc.*, 1998, **120**, 6167–6168; (c) H. Kawai, T. Takeda, K. Fujiwara, M. Wakeshima, Y. Hinatsu and T. Suzuki, *Chem. – Eur. J.*, 2008, **14**, 5780–5793; (d) B. Kahr, D. Van Engen and K. Mislow, *J. Am. Chem. Soc.*, 1986, **108**, 8305–8307.
- 26 (a) S. Grimme and P. R. Schreiner, *Angew. Chem., Int. Ed.*, 2011, **50**, 12639–12642; (b) P. R. Schreiner, L. V. Chernish, P. A. Gunchenko, E. Y. Tikhonchuk, H. Hausmann, M. Serafin, S. Schlecht, J. E. P. Dahl, R. M. K. Carlson and A. A. Fokin, *Nature*, 2011, **477**, 308–311.
- 27 CCDC 1519042–1519049 contain the supplementary crystallographic data for this paper.